MILLIMETER ARRAY
SCIENTIFIC MEMO NO. 6
(1986)

# CIRCUMSTELLAR SHELLS AND EVOLVED STARS

## WORKING GROUP REPORT

Contributors: John H. Bieging - Radio Astronomy Laboratory, University of California Berkeley, David E. Hogg - National Radio Astronomy Observatory, Philip R. Jewell - National Radio Astronomy Observatory, G. R. Knapp - Department of Astrophysical Sciences, Princeton, Stephen P. Reynolds - National Radio Astronomy Observatory, P. R. Schwartz - National Research Lab (Chairman and Editor), Peter Wannier - Jet Propulsion Lab.

## 1. OVERVIEW

Evolved stars and their envelopes are the most natural target for observations with a millimeter-wave array. This assertion is proved by the facts that current millimeter-wave interferometers at Hat Creek and OVRO have been used extensively to study their structure, that a large amount of work on them is conducted with the VLA at centimeter wavelengths, and that they are almost the only use of VLBI techniques in galactic astronomy. Two reasons can be cited for this interest. The study of star-like sources obviously requires high spatial resolution and the ability to map a complex region. If a stellar envelope has dimensions of 10-1000 AU, then at typical distances of a kpc, its angular size will be 1" -0"01. The more important reason, however, is the increasing realization of the importance of these objects in galactic evolution and of the process which produces an extended envelope, mass loss, in the life of many stars. We now know that mass loss accompanies giant branch evolution and modifies stellar evolution both in terms of rates and masses. We are also becoming aware of the presence of a galactic bulge component which is largely composed of stars similar to those in the solar neighborhood which have been assumed to be an extreme case of giant branch evolution with mass loss. Studies of mass loss and of the resultant envelopes seem to show that late type stars are a significant contributor of processes material to the ISM. They could return as much as 0.3 $M_\odot$/yr which would nearly match the star formation rate. If this last case is true, an understanding of these objects and the mass loss mechanism is a prerequisite to analysis of the entire star formation process. Taken to the extreme, late type star evolution and mass loss may be

the key to galactic evolution.

In the following discussion the major scientific issues concerning evolved stars and circumstellar shells will be reviewed as will be some of the current results in this field. A specific millimeter-wave array design is not tested against these issues, but rather a series of experiments for a millimeter-wave array are developed. These experiments are listed in Section 5. The resultant requirements for a millimeter-wave array are given in Section 6 as conclusions.

## 2. ASTROPHYSICAL ISSUES

### 2.1. THE EVOLUTIONARY STATE OF LATE TYPE STARS

Toward the end of their lifetimes, low and intermediate mass ($1\ M_\odot \lesssim M \lesssim 10\ M_\odot$) stars go through a high mass loss phase. As a result, a circumstellar envelope is formed that can often be detected with millimeter-wave spectral line and continuum observations. In general, these stars are cool giants or supergiants or are hotter objects that may be in even more advanced phases of evolution. Several categories of objects can be identified:

1. Classical Mira and semi-regular variables (periods $\gtrsim$ 1 year)
2. OH/IR and carbon stars
3. Objects with warm central stars (Sp = F through B)
4. Planetary Nebulae

Current stellar evolution theory (Iben and Renzini 1983 Ann. Rev. Astron. Astrophys. 21, 271) places stars in categories 1 and 2 in the asymptotic giant branch (AGB) stage of evolution. Category 3 and 4 objects have evolved beyond the AGB. AGB stars are characterized by a degenerate carbon-oxygen core with He and H shell burning zones. They experience episodes of rapid He burning resulting in thermal pulses. A consequence of these thermal pulses is that processed material (c) from the He burning zone may be mixed into the H envelope in a series of "dredge up" phases.

Category 1 and 2 stars lose mass at often very high rates (up to 10-5 $M_\odot$/yr) in nearly continuous mass loss flows or possibly in more episodic outbursts. The process producing mass loss in these stars is not well understood but radiation pressure on grains condensing in their cool, extended atmospheres is suspected. Atmospheric shock waves driven by envelope pulsations may also

contribute. The mass loss flows of these stars can often be detected by a variety of millimeter-wave observations including molecular line spectroscopy, dust, and free-free continuum.

AGB stars are the suspected progenitors of Planetary Nebulae (PN). It has been held that near the end of red giant evolution, the stars' envelopes can be ejected by a sudden cataclysmic event. Alternately, there may be a smooth transition from a mass loss outflow into the PN phase. Current speculation is that there is a point in AGB evolution at which the steady mass loss outflow switches from a "normal" level to a "superwind" level. This increase in the outflow rate may be induced by a pulsation mode switch from first overtone to fundamental mode pulsation. After a sufficient portion of the stellar envelope is blown off the star begins a blue-ward journey across the H-R diagram, which if the star reaches ionizing temperature before the remnant envelope is dispersed, ultimately results in a classical PN.

Certain objects are conjectured to be in the transition between red giant and PN (e.g., GL 2688, IRC+10420, GL 618). A few PNs have neutral envelopes (e.g., NGC 7027, Vy2-2) interpreted as remnants of the red giant envelope circumstellar envelope. Although this picture is appealing, some problems exist: almost all of the transition objects and 50% of PNs have non-spherical envelope morphology, while the envelopes of their supposed progenitors are usually spherically symmetric.

## 2.2. STELLAR MASS LOSS

Mass loss from red giants was inferred from observation of OH, H2O and SiO masers, but is more directly shown by the detection of CO (1-0) and (2-1) emission lines. About 120 stars are known CO sources and as many as 300 are detectable with current technology. Detections are about evenly divided between oxygen and carbon rich objects ($O/C \gtrsim$ or $\lesssim 1$) of all categories from Miras through PN-like objects.

These observations yield well-defined values of the mass outflow velocity and stellar systemic velocity. Line fitting allows the stellar velocity to be determined with great precision, and the average and terminal velocity of the outflow to be estimated. The stellar velocities are of great value when compared with optical and infrared line velocities in analyzing the pulsations of the stellar atmosphere. They can also be used to study the galactic kinematics of the group of stars

to, for example, estimate progenitor masses. Observed outflow velocities are in the range 4-60 km/s with some indication of a correlation with luminosity. By careful analysis of the CO profile the envelope mass and mass loss rate M can be estimated. Mass loss rates in the range 3 x $10^{-8}$ to 3 x $10^{-4}$ $M_{\odot}$/yr are inferred with considerable uncertainties because of the uncertainties of the CO/H2 conversion ratio, distance, and assumed temperature and radial distribution. Oxygen rich stars span this range of mass loss rates while the carbon stars cluster near a few x $10^{-5}$ $M_{\odot}$/yr.

The composition of the stellar envelopes produced by these mass outflows can be estimated for C, N and O isotopes from observation of CO isotope substituted transitions. Some of these results will be discussed in Section 2.3. The gas-to-dust ratio can also be estimated by comparing CO and continuum observations. The gas-to-dust ratio appears nearly constant and is approximately equal to the interstellar value.

Circumstellar chemistry appears to be dominated by photospheric chemistry particularly in carbon stars. It is, therefore, quite different from interstellar chemistry. Large abundances of SiS and carbon rich molecules ($HC_XN$) are seen, but molecular ions are absent.

The morphology and extent of circumstellar envelopes is determined by the dynamics of the mass loss process and by the stellar and interstellar radiation field (ISRF). Stellar envelopes are, thus, an unparalled astro-chemistry and radiative transfer laboratory because: (a) the envelopes' density structure is approximately known, (b) the time of exposure to the ISRF can be estimated, and (c) the distribution of photoproducts (CN, $C_2H$) can also be observed.

Except for a few pathological objects and PN, mass loss from evolved stars appears to be primarily radiatively driven. This conclusion results from the observation that $\dot{M}V/(L/c) = B$ peaks at unity with a scatter of about a factor of 3. Oxygen rich stars usually have $B \lesssim 1$. Stars with $B \lesssim 1$ usually have shorter periods than those with $B = 1$, probably because their envelopes are more tightly bound (and thus have lower mass loss rates). PN are the exception to this rule (i.e., $B \gtrsim 1$) suggesting that the stellar luminosity drops substantially after the beginning of PN formation. Otherwise, the molecular clouds associated with PN and PN pre-cursors are similar to those associated with cool stars.

## 2.3. MASS LOSS AND THE ISM

The total rate of mass loss by late stars could be as large as 0.35 $M_\odot$/yr making them a significant contributor to the cycle of star formation and return of processed material to the ISM. The cores of red giant stars support a variety of H and He reactions which produce the CNO nuclides. If dredge up of neutron rich core material accompanies mass loss, significant consequences to galactic chemical evolution result. Individual stars with CNO abundances which are very different from either solar or interstellar values are observed with prodigious mass loss rates (up to $10^{-4}$ $M_\odot$/yr). Fully 50% of extreme mass loss objects are carbon rich ($C \gtrsim 0$) implying that freshly synthesized carbon enriches the ejected material. The relative abundances of the CNO isotopes are a much more sensitive indicator of the operating nucleosynthesis processes than chemical abundance ratios such as C/O or N/O. Isotope ratios are both sensitive to specific reaction cycles and more easily measured because they have similar physical and chemical properties. Spectroscopically, isotope substituted molecular transitions are usually easily separable, but not separated by large enough intervals to make precision measurements difficult.

CNO isotopes are the products of several different processes: $^{12}C$, $^{16}O$ and probably $^{18}O$ are the products of He burning, and can thus be cycled into the ISM by red giant mass loss or supernovae. $^{14}N$, $^{13}C$, $^{15}N$ and $^{17}O$ are thought to be the products of H burning either by equilibrium CNO cycles or explosive H burning. The relative abundances of these isotopes in the CNO cycle are determined by initial nuclear composition and nuclear reaction cross sections. CNO processed material should have enhanced $^{14}N$, $^{13}C$, and depleted $^{15}N$ and $^{18}O$ relative to the solar abundance. The observable shell abundances depend upon a variety of factors including both the history and activity of the stellar interior, the degree and rate of mixing to the surface, and the mass loss process. For the purpose of determining the effect of red giant mass loss on galactic evolution, the entire history of enrichment by single stars must be studied. It is important to observe objects at all stages of red giant evolution to determine what, if any, effects stellar evolution has upon isotope abundances.

The comparison of red giant predicted and observed abundances with observed galactic abundances is a test of the hypothesis that red giants actually cycle significant amounts of processed

material back into the ISM. Table 2.1 shows the observed abundances of four types of material: solar system, GMCs in the disk $\gtrsim$ 3 kpc from the galactic center (GC), GMC near the GC, and an average in red giants (Wannier 1980 Ann. Rev. Astron. Astrophys., 18, 399, Wannier 1985 in preparation).

Table 1
Isotope Ratios

| Region | $^{17}O/^{18}O$ | $^{12}C/^{13}C$ | $^{16}O/^{17}O$ | $^{16}O/^{18}O$ | $^{14}N/^{15}N$ | $^{32}S/^{34}S$ |
|---|---|---|---|---|---|---|
| Solar | 0.186 | 89 | 2630 | 490 | 272 | 23 |
| Disk | 0.27 | 60 | 2400 | 700 | 333 | 21 |
| Galactic Center | 0.29 | 26 | 900 | 250 | $\gtrsim$ 550 | 18 |
| Red Giants* | 1.6 | 15 | 460 | 545 | $\gtrsim$ 515 | 22** |

* Straight average of available observations
** IRC+10216 only

The solar values represent abundances at the formation of the solar nebula ($\gtrsim 10^9$ years ago) while the disk GMCs probably represent the current disk values. The clouds in the GC probably represent more evolved material which has been subject to more recycling through stars (as evidenced by the higher stellar metallicity and older stellar population and the smaller gas fraction). Although a strict sequence is not proven, some evidence for nuclear processing by red giants is suggested by this data. Red giant processed material may be enriching the ISM in $^{13}$C and $^{17}$O. The large spread in observed red giant abundances however are a problem, as is the essentially identical value of the disk and GC.

## 3. OBSERVATIONAL ASPECTS

Circumstellar envelopes are an intensively studied phenomenon in millimeter-wave astronomy. Current activities and results using high resolution instruments such as the Hat Creek and OVRO interferometers and some of the limited VLBI results are an important guide to their future investigation.

### 3.1. STELLAR MASERS

Astrophysical masers are a valuable but sometimes difficult to interpret probe of the structure and kinematics of high density regions. A complex spectrum of very high surface brightness velocity components is observed. Each velocity component usually originates from a single spatial

spot which is separated from others in a larger masering region. The SiO maser is only observed in the cool, extended envelopes of late type stars and Orion. These late type stars, Mira variables and even more extreme oxygen rich types, are as we noted in Section 2.3 a significant galactic population and lose mass at very large rates. They could be primary source of processed material returned to the ISM. OH and $H_2O$ masers are observed in a few transitions and are usually viewed as test particles in the stellar envelopes but the SiO millimeter spectrum exhibits a rich variety of bright lines in many rotational and vibrational states. The diversity of observable excitation states may make the eventual interpretation of SiO possible so that individual maser spots may tag specific densities of other physical conditions.

Stellar masers do not appear to be strictly coincident in individual stellar envelopes and the SiO masers originate inside the OH maser region. OH and $H_2O$ maser maps are consistent with a picture of emission from different portions of a nearly spherical expanding shell Figure 3.1.1. Only the SiO J = 1-0, v = 1 and 2 masers have been observed with better than single antenna resolution and the maser regions and spots appear to have sizes 10-100 AU. By observing both the distribution and variation of maser structure as a function of several transitions, the base of the mass loss region and the driving mechanism for the outflow may be studied.

Maser excitation is still not understood but the existence of OH, $H_2O$ and SiO masers in the same stars hints at a common mechanism. Infrared pumping via similar vibra-rotation transitions in the intense part of the stellar continuum may be the common factor. SiO with the large number of observable transitions may be the only maser which can be ultimately explained. If so, the absolute coincidence of, or spatial relationships between, different velocity and transition spots must be mapped in detail.

Astrophysical masers may be a statistically significant indicator of stellar mass loss. The size of maser regions correlates with several independent indicators of mass loss (Fig. 3.1.2). Currently this correlation is best for extreme OH/IR star objects, which although important are only a small

Figure 3.1.1 VLA maps of 1612 MHz maser emission from OH127.8-0.0 showing its symmetric shell structure (Bowers, Johnston and Spencer 1983 Ap. J. 274, 733.)

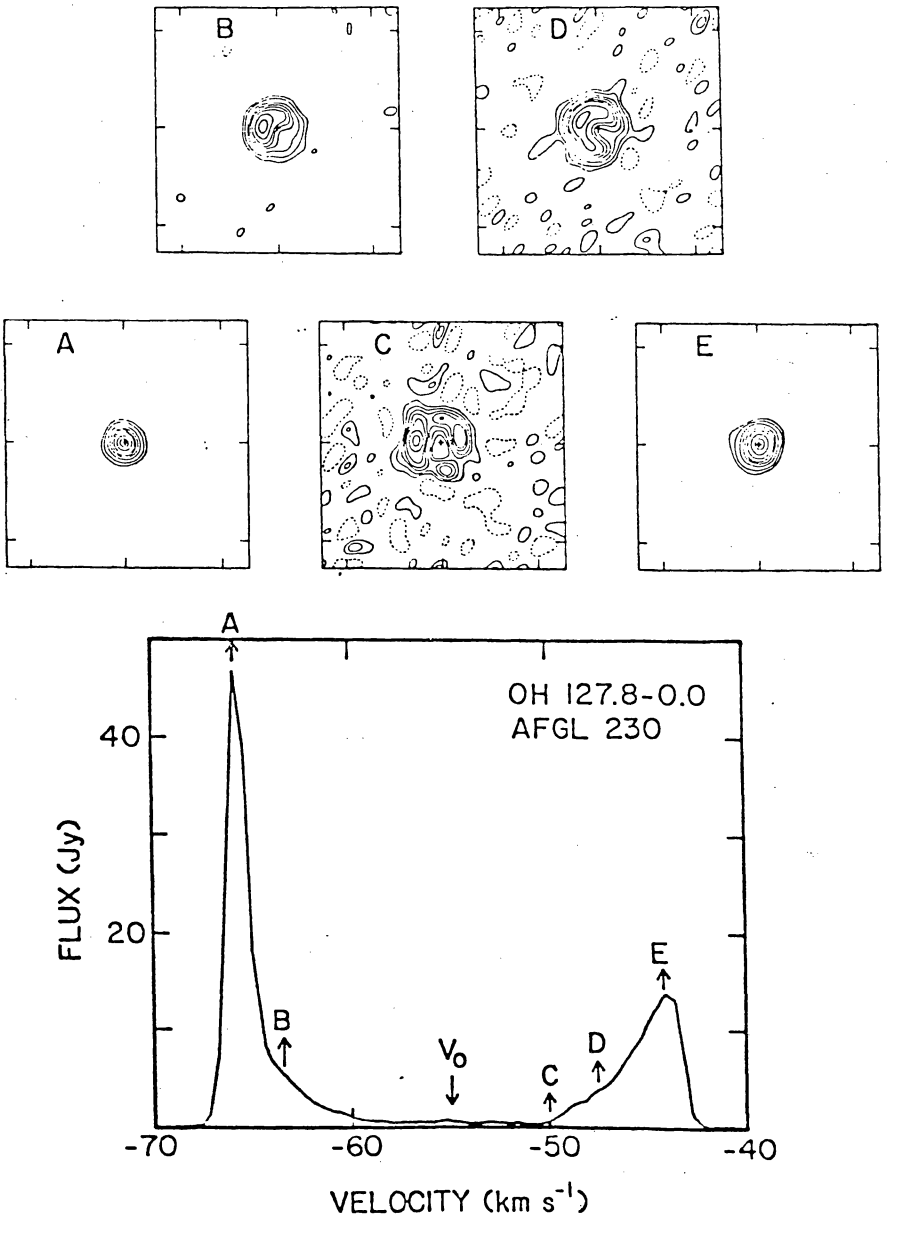

Figure 3.1.2 Radius of the maser region as a function of CO or IR mass loss rate (Bowers 1985, *Mass Loss from Red Giants* M. Morris and B. Zuckerman, eds.)

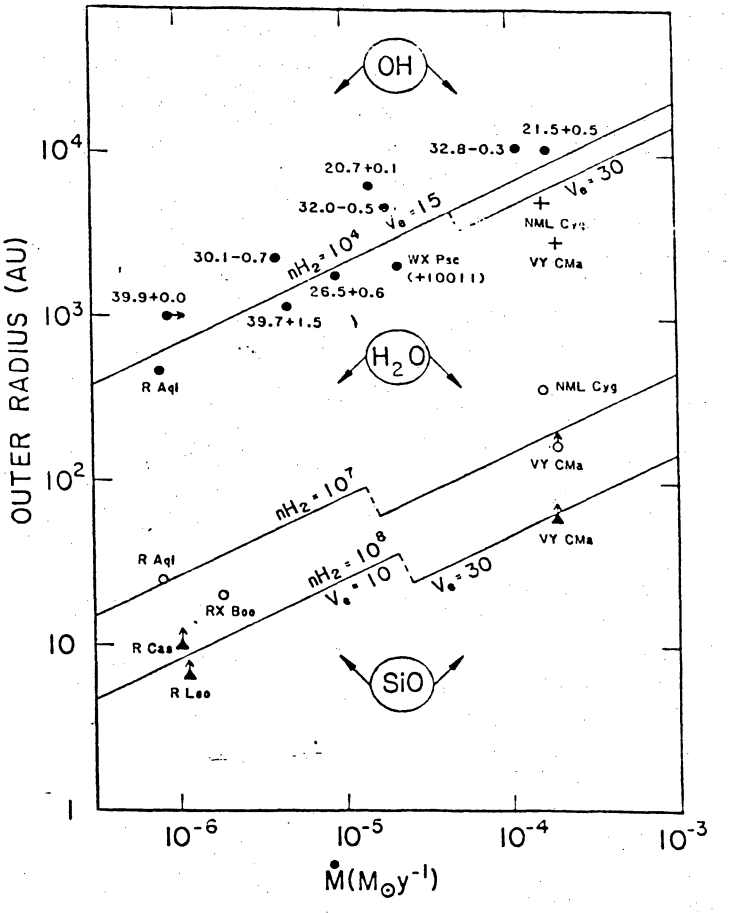

part of the larger picture. The brightness of SiO masers in the "normal" population of Mira variables makes it possible to extend this correlation to a sample of objects which is vastly larger and more significant on a galactic scale.

### 3.2. OBSERVATION OF THE MOLECULAR ENVELOPES OF LATE TYPE STARS

Most of the information concerning the envelopes of late stars discussed in Section 2 was determined from single antenna observations, but at least one object, IRC+10216, has also been studied with the Hat Creek 3-element interferometer. IRC+10216, is approximately symmetric, is strongly centrally peaked and has 6' diameter in $^{12}CO$, but is smaller ($\sim$ 1' in other molecular lines. 11 transitions of 8 species (HNC, SiS, $HC_3N$, $C_2H$, HCO+, $CH_3OH$, $H^{13}CN$ and SO) were observed by Bieging and Rieu (1985 unpublished). Figure 3.2.1 shows an example of the spectra of HNC, SiS and $HC_3N$ simultaneously observed on short baselines (corresponding to 45" and 35" fringe spacings). Even at these spacings, resolution effects are apparent in the spectra implying different sizes and or brightness distributions. IRC+10216 is a carbon star with many detected molecular species and these data show that different species may have different relative abundances and/or excitation as a function of radius from the central star. Observations of a single species, therefore, gives an incomplete picture of the stellar envelope. IRC+10216, it appears, requires imaging on angular scales from 6' to $\lesssim$ 1" in a large number of molecular lines which reflect a range of physical conditions.

An important aspect of the study of molecular envelopes is that because of the high IR flux of the central source, many molecules are radiatively (rather than collisionally) excited. Since the stars are also variable, some transitions should be time variable. SiO masers are, for example, time variable. Bieging, Chapman and Welch (1984) suggested such variability in the HCN 1-0 lines of IRC+10216 based upon a detailed excitation model and fits to their synthesis maps. The effect is best observed when a complete synthesis map can be made at a single epoch and is vital to establishing the relative importance of collisions and radiation in molecular excitation.

### 3.3. MAPPING OF PROTO-PLANETARY NEBULAE

It is believed that as the evolution of the red giant star continues, it will eventually become

Figure 3.2.1 Simultaneous observations of molecular lines in IRC+10216 made with the Hat Creek Interferometer.

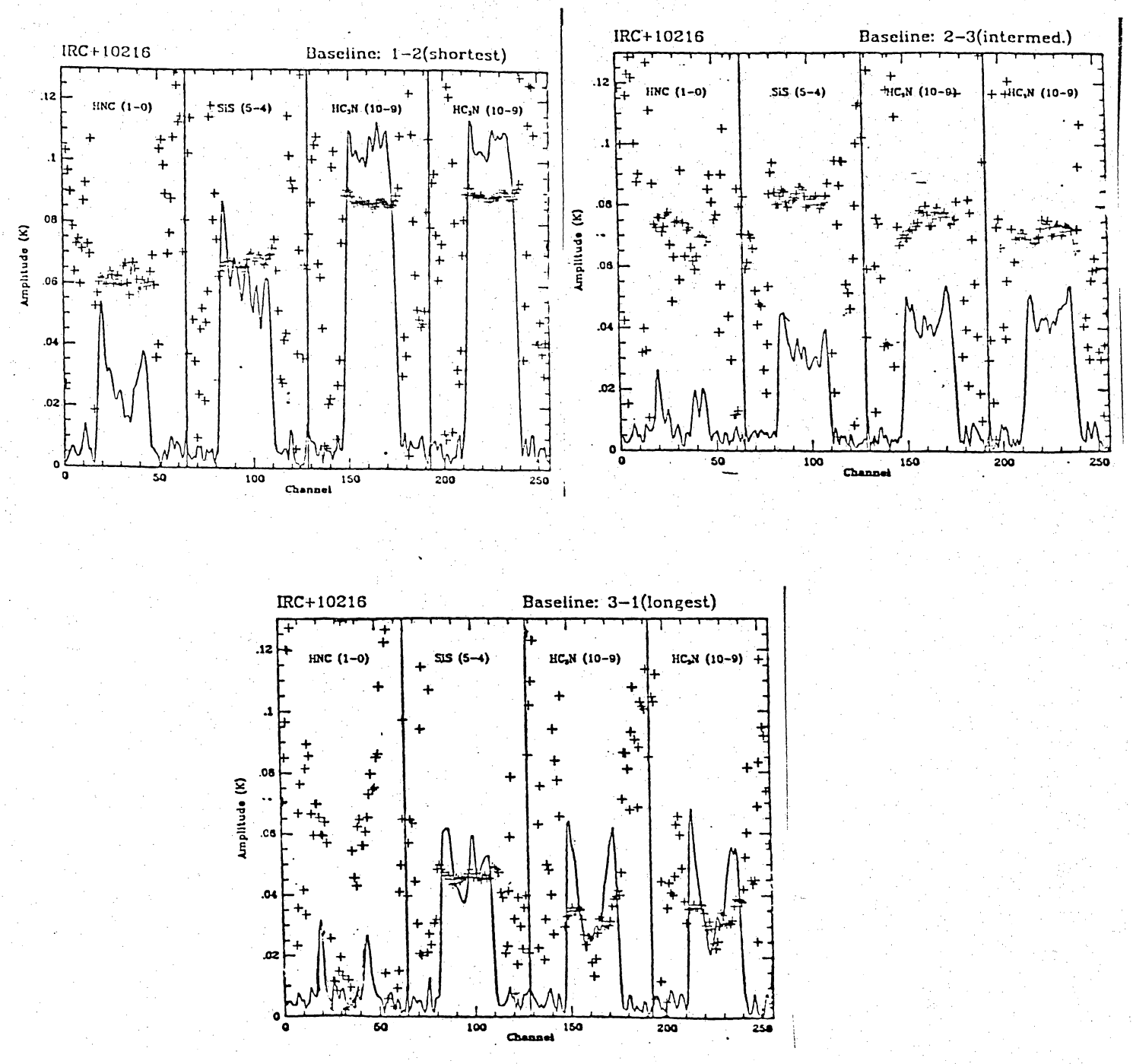

a PN. It will pass from the red giant stage to the PN stage by a short-lived process that is not now understood. By studying the few objects believed to be in transition between the two stages, it may be possible to measure some of the characteristics of the PN formation process.

One prominent object that is probably in transition is the infrared source CRL 618. It is notable for having bipolar reflection nebulosities, between which is situated a strong radio continuum and infrared source. VLA maps by Kwok and Bignell have shown that the central star is surrounded by a compact HII region of size 0.4" x 0.1" (1 x $10^{16}$ cm x 2.5 x $10^{15}$ cm) which perhaps delineates the interaction between the "old" wind of the red giant and the recently developed fast wind of the transient stage. To explore this further, high resolution continuum maps at 1.3 and 3 mm are needed to measure the physical conditions of the ionized region near the star. In addition, the cool molecular envelope of the old wind should be mapped, especially in molecular species which trace regions of high density, to see if the bipolar flow indicated by the ionized material and by the reflection nebulae is being collimated by a dense molecular disk. In the latter regard the first CO maps of CRL 618 are as yet inconclusive, but preliminary maps of HCN of the closely related object CRL 2688 are more encouraging.

An example of high resolution observations of proto-PN is the recent study of CRL 2688 made by Bieging and Rieu (1985 unpublished) with the Hat Creek 3-element interferometer. A total of 10 different transitions of 6 species (HCN, $C_4H$, HNC, SiS, $HC_3N$, $C_2H$) were mapped. Figure 3.3.1 shows a CLEANed map of the average over the HCN line with 5."6 x 7."8 resolution overlaid on an optical photograph. The HCN distribution is clearly non-circular and appears to be aligned with the optical dust lane (Fig. 3.3.2). The HCN is evidently outlining a dense circumstellar disk surrounding the central IR source (i.e., star) but the resolution is not sufficient to determine its thickness. The HCN brightness temperatures are $\gg$ 10 K showing that the disk is not only quite dense ($n(H_2) \gtrsim 10^5$ cm$^{-3}$) but also warm. The molecular line maps of CRL 2688 demonstrate that a picture of a proto-PN can be constructed if complete maps with 1" resolution over a field of view = 1' can be made in several transitions. Velocity information over a wide range, probably at least 100 km/s should also be included.

Figure 3.3.2 Morphology of different CO velocity components in NGC7027 observed with the OVRO interferometer.

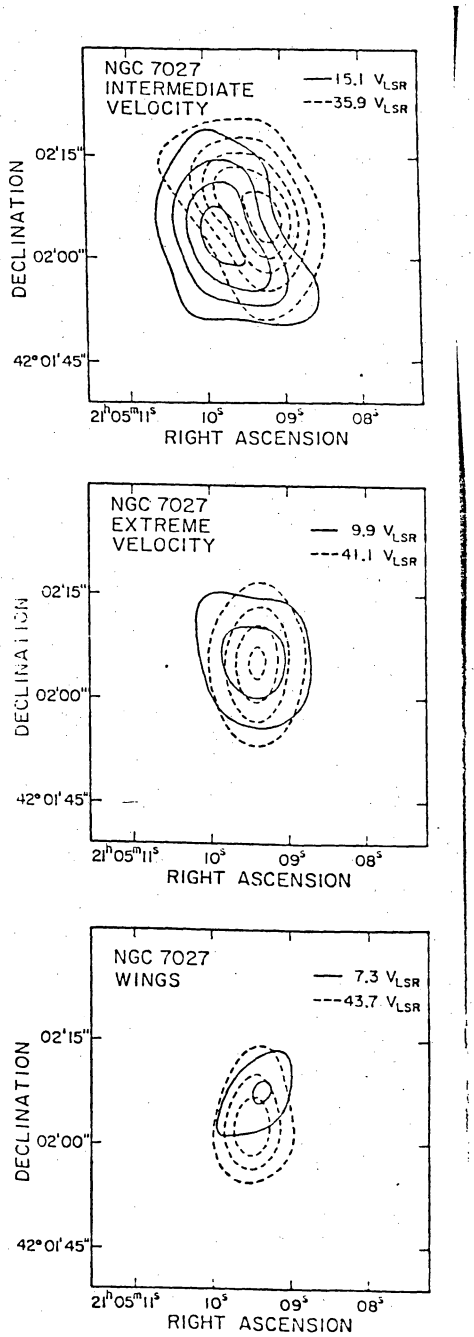

Similar considerations apply to the next stage of evolution in which the PN is well-formed, but there remains a trace of the molecular material from the red giant envelope. There are only a few objects of this type now identified -Vy2.2, NGC 6302, and NGC 7027 are examples–but they offer an important testing ground for theories of evolution. The impact of high-resolution observations is illustrated by the beautiful maps of the CO distribution made with the Owens Valley millimeter interferometer (Fig. 3.3.2 Masson *et al.*Ap. J. 292, 464, 1985). The neutral envelope, presumably the result of the red giant wind is oblate in structure and inhibits the growth of the ionized region (the PN) in the equatorial plane. The CO observations also show the presence of a high velocity gas near the ionized nebula. This gas may be in a shocked neutral shell surrounding the expanding ionized gas. The existence of a shocked region is inferred from the observation of emission from neutral $H_2$.

We anticipate that the millimeter array will be used most extensively in the study of the distribution of molecules in the neutral envelopes and in the shock regions of recently-formed planetaries. Continuum maps will be useful in those cases where the ionized structure is so compact as to be optically thick at wavelengths accessible to the VLA.

### 3.4. THE EVOLUTION OF YOUNG MASSIVE STARS

It is now well established that an important feature of the evolution of O and early B stars is the loss of material in strong, fast stellar winds. The mass loss rate of order $1 \times 10^5$ $M_\odot$ $yr^{-1}$ for B1Ia supergiant is a function of luminosity, suggesting that the wind is driven by radiation pressure. Extreme examples of this phenomenon are the Wolf-Rayet stars which with masses in the range 10-20 $M_\odot$ and mass loss rates of $2 \times 10^{-5}$ $M_\odot$ $yr^{-1}$ are in a short lived stage that may precede a supernova explosion (Abbot, Bieging, Churchwell and Torres, 1986, preprint). The mechanism for the mass loss is not known since the momentum of the wind is large compared to that available from the luminosity of the star. Interest in these stars is great because they may be supernova progenitors. For this reason it is important to get good estimates of properties of the stellar wind, such as the duration of the wind, the total mass lost in the wind, and the extent and chemical composition of the wind-blown shell.

Thermal radio emission has been observed from more than 30 WR stars using the VLA. These measurements have given estimates of mass loss rates for these stars. Similar estimates could be made from radio flux densities measured at millimeter wavelengths. Of more importance, however, is that millimeter wavelength interferometry offers the possibility of exploring in detail the physical conditions in the wind. If the visibility function of the wind can be measured at a number of wavelengths between 20 cm and 1 mm the temperature and density of the wind can be estimated for distances from the star of 50-1500 stellar radii. From these data we can hope to answer the following questions:

1. Is the outflow spherical?

2. Has the outflow reached terminal velocity in distance of $50R_*$?

3. Is the flow isothermal?

4. Are the ions in the flow recombining?

Knowledge of the physical conditions in the wind will provide important constraints on the models of the wind mechanism that have been proposed.

Similar considerations apply to the case of the winds from OB stars, except that they are in general much more difficult objects to observe, because the mass loss rates cover a much broader range than W-R stars. Nevertheless, there are many few stars which are bright at radio wavelengths either because they are close or because they have unusually high rates of mass loss. For these objects millimeter wavelength interferometry will enable exploration of the radial distribution of temperature and density in the wind.

## 4. RELATED ASTROPHYSICAL PROBLEMS

### 4.1. VEGA PHENOMENON AND MILLIMETER-WAVE PHOTOMETRY

The continuum resolution and sensitivity of the projected Millimeter-wave Array will make it a powerful extension and complement to the far infrared and sub-millimeter photometry being planned for the 1990s and to IRAS. The "Vega Phenomenon" is an excellent example of this point. Very large (a = 1 mm) grains orbiting main sequence stars produce a far infrared excess in their spectra. These grains are a permanent relic of the star formation process and are related to the

sun's cometary and planetary system. In Vega this component results in a spectral component with blackbody temperature = 85 K and $S_\nu$ (100 $\mu$m) = 7 Jy. Since the grains are larger than the wavelength, the spectrum is blackbody so that the expected flux at 1.3 mm, 40 mJy, is well above the detection limit of proposed arrays. In fact, the proposed arrays will be about an order of magnitude more sensitive than IRAS for detecting Vega-like objects.

A related project is the photometry of unidentified IRAS 100 $\mu$m objects to determine their spectra and positions. If the unidentified objects have cool dust emission spectra, then all IRAS sources with $S_\nu$ (100 $\mu$m) $\gtrsim$ 1 Jy can be detected with proposed arrays and their positions determined with arc-sec precision. Identifications should follow easily at this positional accuracy (IRAS positions are good to $\lesssim$ 1' so that identifications with distant objects are confused).

4.2. SUPERNOVA REMNANTS

The explosion of the supernova typically results in the ejection of up to the ten solar masses of material into the surrounding medium. These ejecta interact first with ambient circumstellar material, then with the interstellar medium at large, producing a rich complex of phenomena. In addition, if a magnetized neutron star is formed, its energy input may drive a further interaction with the surrounding supernova ejecta.

If the supernova progenitor or its companion produced a stellar wind typical of red giants, the explosion will take place in a relatively dense medium. This interaction results in the acceleration of relativistic particles, perhaps accompanied by turbulent amplification of magnetic fields, with resultant production of nonthermal emission. This is the phenomenon of the radio supernova. Considerably later, the remnant shock wave is interacting with ambient interstellar medium. Again, the collisionless shock wave appears to cause some combination of acceleration of particles and amplification of magnetic field. The detailed physical processes are not well understood. In young remnants, observational evidence suggests magnetic-field amplification at the shock wave, though the plasma physics remains obscure. In older remnants, magnetic pressure may limit the compression in cooling filaments.

In the pulsar-driven (Crablike) supernova remnants the particle acceleration is even more

obscure. However, evolutionary processes cause the initial, presumably pulsar-produced spectrum to develop structure. This structure in the form of spectral steepening makes potentially observable such quantities as the pulsar's characteristic energy-loss time and the mass of material currently interacting with the pulsar's injected bubble of relativistic particles and magnetic field.

The extension to millimeter wavelengths of high-sensitivity imaging capability can be a powerful tool in the investigation of these problems. Radio supernovae become visible first at high frequencies; a powerful millimeter interferometer could detect and identify new supernovae without confusion problems, providing information on the density of the circumstellar medium and the spectrum of accelerated particles. In older remnants, synchrotron-loss effects on particle energy spectra can begin to appear at millimeter wavelengths. In middle-aged remnants such as the Cygnus Loop, optical filaments identify cooling shock waves and are also often coincident with radio filaments. Optical spectra provide information on compression and shock velocity; a break in the radio spectrum of a filament can then give the magnetic field and the energy in particles, allowing a direct determination of the efficiency of the shock at accelerating particles and magnetic field. These effects are not detectable at centimeter wavelengths, and their analysis requires resolution of a few arcseconds or better.

Evolutionary models of Crablike remnants predict the appearance of a spectral break in the millimeter region. Inhomogenities in magnetic-field strength can then appear as structure in spectral-index maps. In the Crab, possible correlations with optical filaments should be investigated. In other Crablike remnants, finding such a break can better determine the evolutionary stage of development, with implications for the ejected mass and the age.

## 5. EXPERIMENTS FOR A MILLIMETER-WAVE ARRAY

The astrophysical issues and growing body of observational experience discussed in the previous sections leads to a group of obvious experiments for a millimeter-wave array. These experiments are perceived as finite observing programs for any potential array and will probably represent the highest priority proposals for such an instrument.

1. Detailed multi-spectral mapping of about 30 C and O rich late type stars at resolutions

1" - 1' to determine the structure, chemistry and excitation of their mass outflows.

2. A survey of about 100 late type stars in various isotopic lines to statistically study chemical and abundance trends over galactic radius and stellar type.

3. Very high resolution ($\lesssim$ 1") multi-molecular mapping of a sample of about 20 proto-PNs to detect asymmetry or characteristic structures.

4. Very high sensitivity and resolution ($\lesssim$ 0.01") maps of dust continuum and selected molecular lines in a small sample of O and C giants to detect the inner and outer boundary of the flows, dust formation radius and dissociation edge.

5. Very high resolution ($\lesssim$ 0.01") mapping of the SiO maser structure of about 50 stars to map out the base of the mass loss outflow in Mira variables.

6. Monitoring of the time dependent structure of radiatively excited molecules in several variable stars.

7. Observation of the total dust continuum in a sample of C and O rich stars to determine total dust mass.

8. Detailed mapping of the HII cores of several proto-PNs.

9. Measurement of the visibility function of Wolf-Rayet stars out to 2 kpc to determine the temperature structure of their outflows.

10. Mosaic maps of about 10 SNRs.

11. Observe the radio turn on of extragalactic SN.

## 6. REQUIREMENTS FOR A MILLIMETER-WAVE ARRAY

The scientific issues and proposed experiments discussed above set certain requirements on a millimeter-wave array. These requirements are listed below.

1. Operating frequencies - 100-1000 GHz, preferred frequency range is 230-345 GHz.

2. Effective area - minimum of 2000 $m^2$ at 230 GHz.

3. Maximum sensitivity mode for continuum observations near 300 GHz.

4. Maximum IF bandwidth ($\gg$ 1 GHz) and facility for spectral multiplexing to allow simultaneous observations of many spectral features.

5. Available resolving power for complete maps from 1' to 0."1 with some facility for even higher resolution. No preferred baseline orientation is required, most likely targets are at declinations $\gtrsim 0^{o}$.